Clinical Chemistry 44:3
591–598 (1998)

Automation and Analytical Techniques

Microchip systems for immunoassay: an integrated immunoreactor with electrophoretic separation for serum theophylline determination

Nghia H. Chiem and D. Jed Harrison*

A glass microchip is described in which reagents and serum samples for competitive immunoassay of serum theophylline can be mixed, reacted, separated, and analyzed. The device functions as an automated microfluidic immunoassay system, creating a lab-on-a-chip. Electroosmotic pumping was used to control first the mixing of 50-fold-diluted serum sample with labeled theophylline tracer in a 1:1 ratio, followed by 1:1 mixing and reaction with anti-theophylline antibody. The 51-nL on-chip mixer gave the same concentration as dilution performed off-chip, within 3%. A 100-pL plug of the reacted solution was then injected into an electrophoresis separation channel integrated within the same chip. Measurements of free and bound tracer by fluorescence detection gave linear calibration curves of signal vs log[theophylline] between 0 and 40 mg/L, with a slope of 0.52 ± 0.03 and an intercept of −0.04 ± 0.04 after a 90-s reaction time. A detection limit of 0.26 mg/L in serum (expressed before the dilution step, actual concentration of 1.3 μg/L at the detector) was obtained. Recovery values were 107% ± 8% for 15 mg/L serum samples.

Micromachining technology has provided a means of fabricating miniaturized, three-dimensional structures capable of performing clinically relevant analyses *[1–5]*. This technology offers promise in developing miniaturized instrumentation with a high amount of automation and rapid analysis times *[2, 5–8]*. Passive devices, in which sample flow is driven by some external means, have been used for treatment of blood or serum *[5, 9]*, measurement of sperm motility *[9, 10]*, coagulation-based immunoassay *[9, 11]*, and as miniature containers for performing the PCR to amplify DNA *[5, 9, 12, 13]*. Most of the successful active devices, in which fluid flow and delivery are driven on-chip, have been based on electrokinetic effects *[2–4, 6–8, 14]*. In these devices, electroosmotic flow has been used to drive fluid flow in complex networks of fluid channels, providing pumping and valving action without the need for moving parts. On-chip chemical reactions followed by separation based on electrophoretic effects have been shown *[15–17]*. Applications of microchip-based capillary electrophoresis (CE)[1] devices to some clinically relevant samples has been shown *[4, 8, 17–20]*, but the integration of several sample preparation steps together to create a lab-on-a-chip for clinical measurements has only just begun *[21]*.

Application of CE to immunoassays is a newly developing field showing considerable promise *[22–24]* and appears appropriate for translation to the microchip CE format *[4, 8, 18]*. The CE immunoassay method uses a homogeneous phase immunoreaction, which is frequently very rapid because of good mass transfer kinetics, followed by a separation step to isolate and analyze the reactants and products. The separation is also very rapid, especially when performed on-chip, because of the very short separation distances. To our knowledge, the reaction of immunoreagents on-chip, followed by on-chip separation, which represents an increased level of automation of the CE immunoassay, has not been demonstrated. In this report, we demonstrate a competitive assay in which on-chip mixing of diluted serum samples with a labeled tracer compound and a selective antibody can be followed by separation and analysis of the components. This result, shown for the drug theophylline (Th), provides confirmation that the integration of several steps to create a lab-on-a-chip for a real, clinical analysis is indeed feasible. We expect that the unique fluid delivery capabilities of the microchip electrophoresis format will provide a novel, important new method for automating

Department of Chemistry, University of Alberta, Edmonton, Alberta, T6G 2G2 Canada.

* Author for correspondence. Fax 403-492-8231; e-mail Jed.Harrison@ualberta.ca.

Received April 28, 1997; revision accepted October 27, 1997.

[1] Nonstandard abbreviations: CE, capillary electrophoresis; Th, theophylline; Th*, fluorescein-labeled theophylline; Ab, antibody; DL, detection limit; and FPIA, fluorescence polarization immunoassay.

immunoassays for use at the point-of-care in the clinical environment *[4, 8, 25]*.

Materials and Methods

MATERIALS AND REAGENTS

Borofloat glass was from Paragon Optical. Th and Tricine were from Sigma Chemical Co. Fluorescein-labeled Th (Th*) and anti-Th antibody (Ab) were part of the Abbott TDx reagent set (Sigma). NaOH and NaCl were from BDH (Fisher Scientific). Tween 20 was from Aldrich. Human serum was a gift from Bio-Rad. All chemicals were reagent grade; doubly distilled water was used for all solutions. Most solutions were filtered with 0.22-μm pore-size filters (Millipore); small volumes were filtered with Micropure separators with 0.22-μm pores (Amicon). Microconcentrators with various molecular mass cutoffs were also from Amicon.

The "Tricine" buffer contained 50 mmol/L Tricine adjusted with sodium hydroxide to pH 8.0, 0.1 g/L Tween 20, and 26 mmol/L NaCl *[4]*. Tricine buffer was filter-sterilized (0.22-μm-pore filter) and was used within 3 days for sample dilution and separation.

DEVICE FABRICATION

Devices were fabricated at the Alberta Microelectronic Centre in 7.6 × 7.6 cm square Borofloat glass by using a microlithographic patterning technique and an HF/HNO_3 acid etchant mixture, as described previously *[4, 16]*. The chip layout is shown in Fig. 1. The solution reservoirs are numbered from 1 to 7 for identification. The line thicknesses represent the relative widths of the channels, with other dimensions given in Table 1. To allow for easy calculation of electric field strengths in each channel, the lengths of all channel segments are also given in Table 1 and expressed in terms of an equivalent length of a channel 52 μm wide *[26]*. Channel segments from reservoirs 5 and 6 met at junction J1. When the solutions flowed in the directions indicated by the arrows, the segment between J1 and junction J3 served as a mixer for the two solutions from reservoirs 5 and 6. The mixture from J1-J3 was then mixed with the solution from reservoir 7 in segment J3-J4. The inset magnification shows the double-T injector *[27]* region, with a center-to-center length between the two arms of the T of ~100 μm and a volume of ~100 pL.

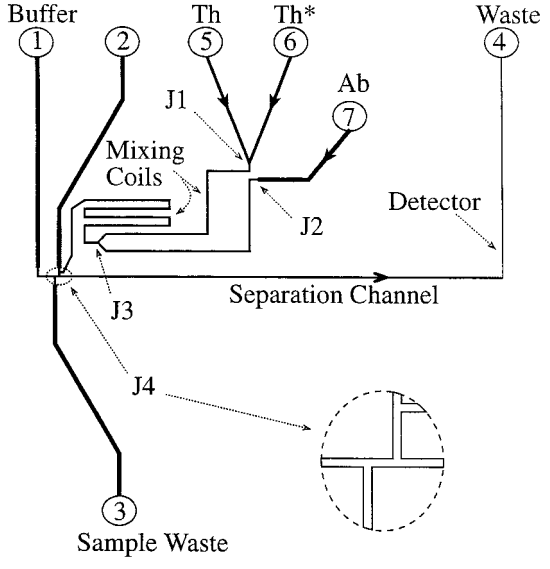

Fig. 1. Device layout for competitive immunoassay showing numbering scheme for solution reservoirs and junctions.

Differing line thicknesses indicate relative channel widths; actual dimensions are given in Table 1. The segment joining J1 to J3 was used for mixing of antigen (Th) and tracer (Th*) solutions. The segment J3 to J4 was used to mix the Ab with the antigen and tracer. The double-T injector is shown in the *inset*. The drawing is not to scale.

INSTRUMENTATION

Some modifications were made to the computer-controlled power supply and relay arrangement described previously *[4, 16]*. Only a single 30-kV power supply (Spellman Model CZE 1000R) and two 30-kV Kilovac double-throw relays were used to operate the chip, by using the scheme indicated in Fig. 2. Laser-induced fluorescence with excitation at 488 nm was used. Emission was measured with a ×25, 0.35 N.A. microscope objective, an 800-μm pinhole, an Omega Optical 508–533 bandpass filter, and a photomultiplier tube as described previously *[4]*.

COMPETITIVE IMMUNOASSAY AND CHIP OPERATION

For competitive Th assays, serum Th calibrators from the TDx calibrator kit (0, 2.5, 5.0, 10, 20, and 40 mg/L) were used as received. Th (Sigma) stock solutions were 1 g/L in water. Samples were made by adding Th stock to human serum to give solutions 10, 12.5, and 15 mg/L in Th. Calibrator or sample solutions were then diluted 50-fold in Tricine buffer. Solution T, containing the Th* tracer, was diluted with the Tricine buffer in a 1:1 ratio (by vol.).

Table 1. Dimensions[a] of channels in device.

			Length, mm	
Segment connecting	To	Width, μm	Actual	Equivalent
Reservoir 5	Junction (J1)	116	13.46	5.69
Reservoir 6	Junction (J1)	116	13.46	5.69
Junction (J1)	Junction (J3)	52	26.50	26.50
Reservoir 7	Junction (J2)	236	13.49	2.74
Junction (J2)	Junction (J3)	52	26.50	26.5
Junction (J3)	Junction (J4)	52	81.63	81.63
Junction (J4)	Reservoir 4	52	81.11	81.11
Reservoir 1	Junction (J4)	236	26.00	5.28
Junction (J4)	Reservoir 3	236	36.34	7.38

[a] Device etched 13 μm deep. Cross-section of channels is approximately trapezoidal, with the largest width reported in column 3. The actual lengths of the channel segments are given in column 4, and their corresponding lengths in terms of a channel 52-μm wide are given in column 5, using $l_{eq} = l_{true}\, A_{52}/A_{true}$, where l_{true} is length and A_{true} is cross-sectional area, A_{52} represents a 52-μm wide cross-section, and l_{eq} is the equivalent length *[26]*.

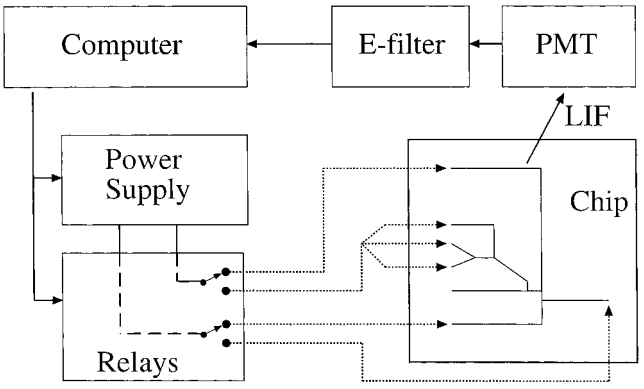

Fig. 2. Instrument setup showing relays and voltage connections to the chip reservoirs.

Only a single power supply and two double-throw relays were used to toggle between different reservoirs. Laser-induced fluorescence (*LIF*) and microscope collection optics were used to detect fluorescent species directly on-chip.

Solution S, containing anti-Th Ab, was dialyzed and reconstituted in the Tricine buffer as described previously *[4]*; 2.5 μL of this solution was then further diluted with Tricine buffer to 40 μL before use.

Chips were initially filled with buffer by introduction into reservoir 1, letting capillary action distribute the solution through all of the channels. Other reservoirs were then filled with the appropriate solution by using a 1-mL syringe with a 20- or 22-gauge needle. Diluted Th sample or calibrator (10 μL), Tracer Th*, and anti-Th solution were added to reservoirs 5, 6, and 7, respectively, as indicated in Fig. 1. Tricine buffer was added to all other reservoirs. The channels were flushed with the reagents by applying the injection step voltage scheme (see below) for at least 2 min. When filling the reservoirs, care was taken not to trap bubbles in them. No difficulties with bubbles in the channels were observed when following this procedural sequence. During sample exchange, only the sample solution in reservoir 5 was replaced, by removing solution from the reservoir with a syringe, followed by three rinses with 6–10 μL of the new sample, then a final addition of ~8 μL. The channels inside the chip were then flushed by using the injection mode for 2 min. Repetitive tests confirmed that there was no carryover or memory effect. The amounts of reagents and buffer in other reservoirs were replenished with the appropriate solution when required.

Figure 3A illustrates the injection scheme. Sample reservoirs (5, 6, and 7) were connected to ground, while sample waste (3) was connected to a negative high voltage (−3 to −6 kV). The samples were electroosmotically pumped in the direction indicated by the arrows by using the applied voltage. On-chip mixing of the solution streams and reaction of reagents took place in the mixing coils. The channel segment between junctions J1 and J3 was used to mix the antigens (Th and tracer), whereas the segment between J3 and J4 was used to mix the antigens with the antibody. The mixed solution passed through the

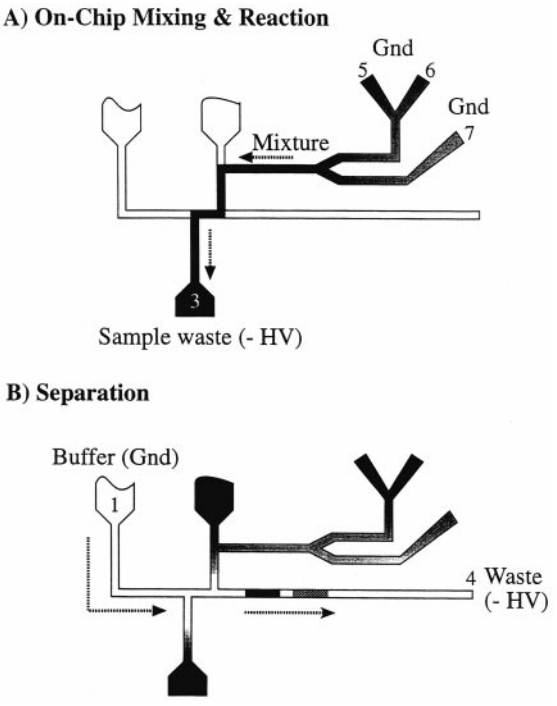

Fig. 3. Electroosmotic pump and electrophoretic separation.

(*A*) Solutions of Th, Th*, and Ab in reservoirs 5, 6, and 7, respectively, were electroosmotically pumped along the *shaded area* by applying electrical ground (*Gnd*) to these reservoirs and −3 to −6 kV (−HV) at *Sample waste* (reservoir 3). This forms a plug of the mixture at the double-T. (*B*) The reagents and products were separated by switching ground (*Gnd*) to reservoir 1 and −6 kV to the separation waste (*4 Waste*, reservoir 4).

double-T injector, thereby forming a plug of mixed sample and Ab ~100 μm long (~100 pL).

Figure 3B illustrates the separation step. Both relays were switched so that the separation buffer (1) and waste reservoir (4) were at ground and −6 kV, respectively, while the other reservoirs were disconnected. The reactants and products within the injected plug were separated along the separation channel and typically detected 56 mm downstream. During separation, sample mixtures were stationary in the mixing coils. In the usual sequence, 30–120 s was required for sample exchange in the sample reservoir, 2 min was allowed for flushing of the reaction and sample channel manifold by using the injection mode, and then separation of the sample plug at the double-T was initiated and continued for 1 min. A new plug could then be formed in a 3-s injection step, followed by another 1-min separation. In this way, the first reaction time was ~30 s (the transit time of the mixing channel), and reaction times were incremented in 1-min steps.

We have estimated the detection limit (DL) for Th by determining the Th concentration needed to increase the normalized Th* peak area to a value 3 SD in noise background larger than the value obtained in a sample with no Th. Noise was estimated as the SD in five replicate area measurements at 0 Th. The estimate of DL was obtained by linear extrapolation of the results for a 20-μg/L Th sample, which corresponds to a concentration

of 5 μg/L in the separation channel, given a 4-fold dilution factor on-chip. The Ab solution, S, was prepared by diluting a 1.5-μL aliquot to 40 μL to ensure that Th* would be in excess.

Results and Discussion

The mixing manifold illustrated in Figs. 1 and 3 was designed to premix sample and Th* tracer in a 1:1 ratio and then mix the resulting solution with Ab, also in a 1:1 ratio. The intention was to apply the same potential to each reservoir and let the geometry of the channels control the mixing ratios. The efficacy of the diffusion-based mixer, the speed of the immunoreaction on-chip, and the performance of the chip for assays of Th in serum samples is outlined below.

MIXING DILUTION RATIO

The volume flow rate of solution at each of the junction points in the mixing manifolds was designed to be equal. The two channel segments between reservoirs 5 and 6 and junction J1 were designed to have equal resistivities and equal cross-sectional areas at the junction to give 1:1 mixing *[26]*. To obtain 1:1 mixing at junction J3, the segment between reservoir 7 and J3 was designed to have a resistivity equal to the combined resistance of the channels between reservoirs 5 and 6 and junction J3. The cross-sectional areas of the two mixing channels at J3 were again equal. Fig. 4 shows electropherograms resulting from on-chip dilution of Th* at the J3 mixing point. In the left electropherogram, reservoirs 5, 6, and 7 contained the same Th* solution; in the right electropherogram, reservoir 7 contained buffer instead. The latter configuration should give a 50% dilution of the Th*. Mixing was effected with −6 kV applied to sample waste reservoir 3 to create a sample plug at the double-T junction, while separation was performed with −6 kV applied between reservoirs 4 and 1, as described in Fig. 3 and *Materials and Methods*. In Fig. 4, left, the area under the Th* peak was 490 ± 9 mV · s [mean and SD for four replicates (n)], whereas on the right, dilution resulted in an area of 236 ± 4 (n = 7). This corresponds to a Th*:buffer ratio of 48.2% ± 1.2%.

Mixing on- and off-chip was also compared. With sample present in reservoir 5 and buffer in reservoirs 6 and 7, a 4-fold dilution of Th* was expected when it reached the double-T injection port at J4. A Th* sample diluted on-chip with buffer gave a peak area of 729 ± 29 (n = 3). The same Th* solution, diluted 4-fold off-chip and introduced through reservoir 2 to the double-T injector so that there was no dilution on-chip, gave a value of 707 ± 42 (n = 5). The ratio of the dilution achieved on-chip to that off-chip was thus 103% ± 7%. Because the second mixer gave a dilution of 48.2%, this meant the first mixer favored reservoir 5, giving a mixing ratio of reservoirs 5 to 6 of 53.4% ± 4%. In this study, we used a simplified potential delivery system, with a single fixed voltage applied to each of the delivery reservoirs, but greater control of mixing is clearly possible if the potentials on each of those reservoirs is varied *[3, 14, 26]*. Consequently, slight differences in mixing ratio between design and result can be readily compensated.

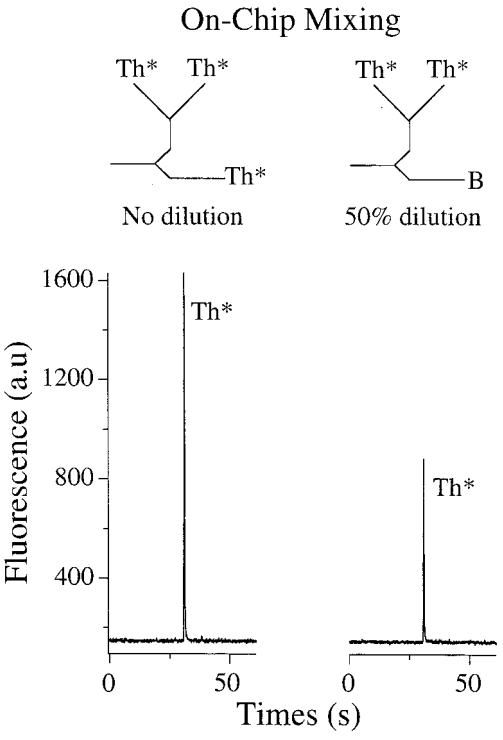

Fig. 4. On-chip dilution of tracer Th* as detailed in the text.

On the *left*, Th* was present in reservoirs 5, 6, and 7 and was loaded into the double-T injector at −3 kV. On the *right*, the Th* solution in reservoir 7 was replaced with buffer, leading to a 1:1 dilution of Th* at the double-T injector during loading. For separation and detection, a pH 8.0 Tricine buffer was used, with 6 kV between reservoirs 1 and 4. *a.u.*, arbitrary units.

DIFFUSIONAL MIXING DESIGN ISSUES

The immunoreagents must be uniformly mixed with the sample before analysis of the reaction products takes place. Dispersion of the reactants must be driven by diffusion, given that the flow conditions on-chip gave low Reynolds numbers *[28]*. To this end, we designed narrow, long mixing coils to allow the species to have sufficient time to uniformly disperse across the channels. The residence time of Th or Ab is defined here as the time the molecules spend in the mixing coil before they are injected for separation. For continuously flowing streams, residence time of a species can be determined from the length of the mixing coil and the flow velocity in the channel.

The velocity of a molecule, ν, can then be determined from the method of Jorgenson and Lukacs *[29]*:

$$\nu = \mu E \quad (1)$$

where μ is the overall mobility of the species and E is the electric field in the channel segment of interest. From the separation data for a mixture of Th* and anti-Th, the mobilities obtained for Th* and the IgG-Th* complex were

2.84 and 4.45 × 10^{-4} cm^2/V·s, respectively. For the −6-kV injection voltage we typically used, the calculated fraction of the voltage drop across the mixing coil J3-J4 was 0.785 or 4.709 kV, giving E = 577 V/cm. The potential between junctions J1 and J3 was 0.762 kV, giving 28.8 V/cm. The calculated velocity for Th* in the 26.5-mm premixing coil J1-J3 was 0.82 mm/s, and under continuous-flow conditions, its residence time was 32 s. In mixing coil J3-J4, the Th* velocity would be 1.64 mm/s, requiring 50 s to travel the 81.6 mm to the injection port. The IgG-Th* complex migrated at a rate of 2.57 mm/s, giving a 32-s residence time in the J3-J4 mixing coil. Previous studies have indicated the free Ab will migrate at a similar rate, although likely somewhat faster *[4, 22–24]*.

Knowing the time each species spends in the mixing channel, we can estimate the time and channel length required for diffusional dispersion downstream of the junctions. Crank *[30]* provides a solution to the initial-boundary value problem of diffusion for a finite system, where a species is initially confined to one-half the width of a channel and then is allowed to diffuse across the full channel:

$$C(x,t) = \tfrac{1}{2}C_0 \sum_{n=-\infty}^{\infty} \left\{ \operatorname{erf} \frac{h + 2nw - x}{2\sqrt{(Dt)}} + \operatorname{erf} \frac{h - 2nw + x}{2\sqrt{(Dt)}} \right\} \quad (2)$$

where x is the location across the channel of width w (52 μm), t is the diffusion time, $C(x,t)$ is the concentration at any given x and t, C_0 is the initial concentration before diffusion (t = 0), n is an integer, h is the portion of the channel width that the species was initially confined to, and D is the diffusion coefficient. This expression was numerically evaluated by using a program written in HiQ script language (National Instruments), with summation taken over the first seven terms (other terms were <0.0025% of the total sum).

Diffusion of IgG molecules initially confined to one-half of the width of the mixing channel was calculated by using Eq. 2, giving the results shown in Fig. 5. Because of its small diffusion coefficient of 4.0 × 10^{-7} cm^2/s *[31]*, IgG requires a long time to become uniformly dispersed across the 52-μm-wide mixing channel. With 6 kV applied, the 81.6-mm-long mixing coil J3-J4 (capacity, 51 nL) allowed sufficient mixing to give only a 1% variation in concentration across the channel under continuous-flow conditions (32-s residence time). (This calculation does not take into account the effect of immunoreaction on the diffusion process, which would tend to speed the time of mixing by increasing the concentration gradient across the channel.)

A similar analysis can be applied to Th dispersion. Lacking the diffusion coefficient for Th or Th*, we used a value reported *[6]* for fluorescein of D = 3.3 × 10^{-6} cm^2/s, which should be similar to that of fluorescein-labeled Th*. Calculation shows that small molecules such as Th or fluorescein will be uniformly dispersed across a 52-μm-wide channel (a 1% concentration variation across the channel) in ~4 s. For the first mixer between J1-J3, with a velocity of 0.82 mm/s, a length of 3.3 mm is required. Consequently, the 26.5-mm length between J1 and J3 (capacity, 16 nL) allowed for more than adequate premixing of the antigens before they met with the antibody solution at J3. For the second mixer from J3 to J4, the velocity of 1.64 mm/s means that a 6.7-mm length is required to uniformly disperse Th across the channel. Because the dispersion of Th and Th* is much faster than that of IgG, this calculation suggests that the second mixer may be unnecessarily long.

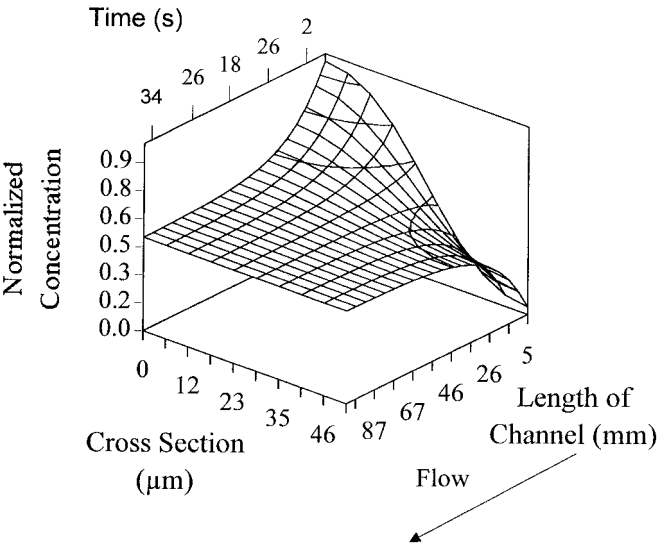

Fig. 5. Plot of concentration of IgG as it diffuses across a 52-μm-wide channel, initially entering from the *top right* side, occupying one-half of the channel.

Eqs. 1 and 2, with D = 4.0 × 10^{-7} cm^2/s and a linear velocity of 2.57 mm/s, were used to calculate the diffusion profiles downstream of intersection J3.

IMMUNOREACTIONS ON-CHIP

Figure 6 shows electropherograms obtained for on-chip competitive immunoassays of serum Th. Mixing was performed at −6 kV under continuous-flow conditions to give ~32-s reaction times, followed by separation at −6 kV. The lowest trace, showing Th* as a single fluorescence peak at ~30 s, was obtained by injection of Th* solution through reservoir 6 and buffer through reservoirs 5 and 7. The central electropherogram was obtained following on-chip mixing of a diluted blank Th (0 mg/L) serum sample in reservoir 5 with tracer Th* from 6, then with anti-Th from 7. The Th* was completely bound to anti-Th to form complexes, which were detected as a new pair of partially resolved peaks at ~18 s as described previously *[4]*. Competitive assays were achieved by replacing the blank sample in reservoir 5 with diluted serum Th solution. In forming complexes, Th in the sample competes with tracer Th* for a limited amount of the antibody in the mixture:

$$\text{Th} + \text{Ab} + \text{Th}^* \Leftrightarrow \text{Ab-Th} + \text{Ab-Th}^* \quad (3)$$

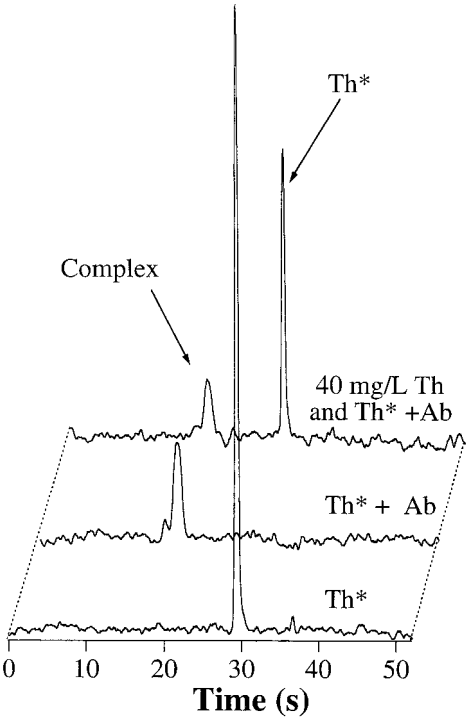

Fig. 6. Electropherograms of the competitive Th assay with on-chip mixing of reagents.

The *lowest trace* is a result of buffer in reservoir 5, Th* in reservoir 6, and buffer in reservoir 7; *middle trace,* buffer in reservoir 5, Th* in reservoir 6, and Ab in reservoir 7; *top trace,* 40 mg/L Th sample (before off-chip 50× dilution) in reservoir 5, Th* in reservoir 6, and Ab in reservoir 7. Buffer and separation conditions were the same as for Fig. 4. All curves are plotted with the same arbitrary fluorescence scale, with a horizontal offset of the baseline for clarity.

The competition leads to an increase in signal for free tracer Th* and a decrease in the Ab-Th* complex, as shown in the top electropherogram. The separation was completed in <1 min; the bound Th*-Ab complexes were well resolved from the free Th*, and the peak areas were easily quantified (see below).

The extent of immunoreaction before the analysis step is clearly critical to quantitative analysis. The chip can be operated in continuous-flow mode during the reaction stage. However, it is also possible to increase reaction times by using it as a stop-flow mixer, allowing incubation in the mixing coil while there is no flow in the mixer. The volume ratio of the second mixer to that of the injector port (51 vs 0.15 nL) means there will be enough reacted sample available. Fig. 7 shows the effect of cumulative mixing time on the distribution between free and bound Th* in a series of competitive assays with serum Th calibrators at 21 °C. Remaining unreacted Th*, normalized to the total fluorescent Th* and injected as described previously *[4]*, is plotted as a function of total mixing time. The results show that the competitive immunoreaction is nearly complete in the first 1.5 min of mixing. A slight continued decrease in free Th* with increased mixing time suggests that the reaction continues at a slow rate for an extended period. Earlier reports indicate the

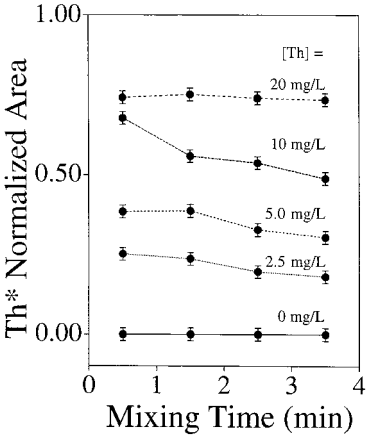

Fig. 7. Stop-flow study of the effect of mixing time on the amount of free, unreacted Th* in the presence of Ab and the indicated amounts of unlabeled Th (concentrations reported as the value before 50-fold dilution off-chip).

The mixed Ab, Th*, and Th solutions were allowed to sit in the channel segment between J3 and J4 for various periods. The shortest mixing time corresponds to the minimum possible residence time, given the velocity of flow with −6 kV applied to the sample waste reservoir. *Error bars* show the SD of four replicates.

Abbott TDx system, based on a fluorescence polarization immunoassay (FPIA) with these same reagents, allows 15 min for incubation at room temperature or 3 min at 35 °C *[32]*. Control of the on-chip reaction time should lead to reproducible results, even if complete reaction has not occurred, although raising the temperature of the chip to reach equilibrium quickly is equally feasible.

COMPETITIVE TH ASSAYS ON-CHIP

Figure 8 shows a calibration curve obtained from a series

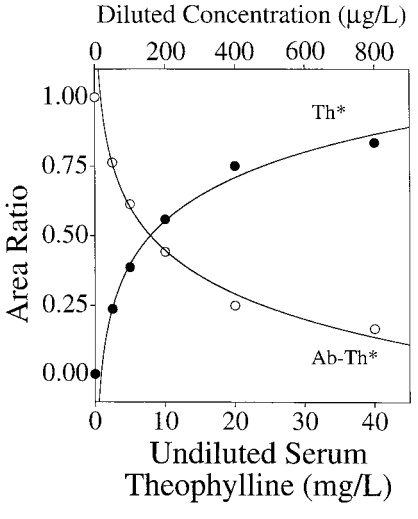

Fig. 8. Calibration curve of normalized peak area for free Th* (●) and Ab-Th* complex (○) vs concentration of Th in 50-fold-diluted serum calibrators (*upper axis*); the *lower axis* shows Th concentrations as they were in serum calibrators before 50-fold dilution off-chip.

Buffer and separation conditions were the same as for Fig. 4; the reaction time was 90 s. Each point is the mean of four replicates. *Error bars* to show ±SD are slightly smaller than the data points. *Solid lines* are fits to a log function; see text.

of separations in which various concentrations of diluted serum Th calibrators were mixed on-chip with the tracer, Th*, and anti-Th solutions. The chip was operated in stop-flow mode, allowing reaction times of 32, 90, 150, and 210 s. Fig. 8 shows a plot of normalized peak area for Th* vs Th calibrator concentration for a 90-s reaction time. A plot of normalized peak area vs log [Th] was linear (slope = 0.52 ± 0.03, intercept = −0.04 ± 0.04, r^2 = 0.988) and allowed calculation of the solid line shown in Fig. 8. As expected from Fig. 7, the slopes varied slightly for different reaction times, and the average values for all reaction times were: slope = 0.54 ± 0.03, intercept 0.003 ± 0.04. The lower abscissa of Fig. 8 shows the original concentrations of Th in the serum calibrators, whereas the upper abscissa shows the concentrations of the calibrators at the stage they were added to reservoir 5. (Dilution of calibrators and serum samples is a standard step with these reagents in the Abbott TDx FPIA; therefore, it was adopted in the present procedure to ensure viable comparison.) The calibration curve covers the important clinical range of 10–20 mg/L for serum samples. It is similar to those obtained with on-chip analysis of off-chip mixed samples *[4]* or with the FPIA method *[32]*.

The recovery of Th from supplemented human serum samples, run over a 2-day period, was determined by using calibration curves obtained with the Th calibrators run on a single day. Human serum samples with Th at 10, 12.5, and 15 mg/L were found to have 9.7 ± 0.7, 12.9 ± 1.0, and 16 ± 1.2 mg/L, respectively (mean and SD over four replicate injections) for data at 90-s reaction time. When data from all reaction times were averaged, the precision of the recovery results was poorer by 40%, likely because of the different extent of reaction seen at different Th concentrations (Fig. 7). The precision for on-chip mixing at 90-s reaction time is similar to that we obtained with off-chip mixing *[4]*. Careful monitoring of the mixing time in both calibrators and sample testing is required to achieve this but is not difficult given the computer control used to run the chips.

The absolute DL for a solution within the separation channel of the chip was determined to be 1.3 μg/L by using the method described in *Materials and Methods*. This is consistent with the value of 1.25 μg/L that we reported previously *[4]* for off-chip mixing with separation on-chip. Under the conditions used to determine the DL, the percentage of Th* bound in the absence of Th was 76%, whereas the percentage of Th* bound at the Th DL was 70%. Because the present chip performs a 4-fold dilution, the minimum concentration that can be placed in sample reservoir 5 is 5.2 μg/L. Given the 50-fold dilution step performed before the samples and calibrators are introduced to the chip, the on-chip reaction and separation system provides a DL of 0.26 mg/L for undiluted serum. This value is similar to the 0.4 mg/L reported for Th assay by FPIA *[33]*, serving to illustrate that DL values are not sacrificed by performing the on-chip immunoassay.

We did not have any difficulty with sample carryover issues with this on-chip assay. The sample exchange described in *Materials and Methods* proved adequate, so that devices could be reused for many months. Because this Th assay uses 50-fold-diluted serum samples and Th does not adsorb strongly onto glass, limited or no carryover might be expected. More-difficult assays or more-dilute samples may demand disposable devices. Although glass devices may prove to be disposable, the recent work on plastic capillary electrophoresis devices *[34, 35]* establishes that alternative, inexpensive materials will be available for single-use devices.

In conclusion, this study has illustrated that integration of several sample-processing steps with CE-based separation of solution components is feasible. Performing reagent mixing with diluted serum samples, immunological reaction, and separation together on one monolithic device makes it clear that entire groups of laboratory steps used in clinical analyses can be integrated. The performance of the device is comparable with conventional instrumentation; therefore, no sacrifice is made by integrating. In the future, the ability to work with blood or serum samples directly within the chips would be another important development. Nevertheless, our results serve to demonstrate the rapid analysis times possible and the amount of automation that can be achieved within the chip. Such devices could form the basis of an automated sample-treatment system to be located at the point-of-care in the clinical and hospital environment, able to provide rapid reporting of critical analytes in emergency situations.

We thank the Natural Sciences and Engineering Research Council of Canada, Defense Research Establishment Suffield, and the Alberta Microelectronic Centre for support. N.H.C. thanks the Alberta Microelectronic Centre for a graduate stipend and the University of Alberta for a Dissertation Fellowship. We thank M.R. Suresh and M. Palcic for helpful discussions related to immunoassays and M. Palcic for the use of various equipment. We are grateful to G. Fitzpatrick and staff at the Alberta Microelectronic Centre for assistance in device fabrication.

References

1. Shoji S, Esashi M, Matsuo, T. Prototype miniature blood gas analyser fabricated on a silicon wafer. Sensors Actuators 1988; 14:101–7.
2. Manz A, Fettinger JC, Verpoorte E, Lüdi H, Widmer HM, Harrison DJ. Micromachining of monocrystalline silicon and glass for chemical analysis systems: a look into next century's technology or just a fashionable craze? Trends Anal Chem 1991;10:144–9.
3. Harrison DJ, Fluri K, Seiler K, Fan Z, Effenhauser CS, Manz A. Micromachining a miniaturized capillary electrophoresis-based chemical analysis system on a chip. Science 1993;261:895–7.
4. Chiem N, Harrison DJ. Microchip-based capillary electrophoresis for immunoassays: analysis of monoclonal antibodies and theophylline. Anal Chem 1997;69:373–8.

5. Cheng J, Fortina P, Surrey S, Kricka LJ, Wilding P. Microchip-based devices for molecular diagnosis of genetic diseases [Review]. Mol Diagn 1996;1:183–200.
6. Harrison DJ, Manz A, Fan Z, Lüdi H, Widmer HM. Capillary electrophoresis and sample injection systems integrated on a planar glass chip. Anal Chem 1992;64:1926–32.
7. Manz A, Harrison DJ, Verpoorte E, Widmer HM. Planar chips technology for miniaturization of separation systems: a developing perspective in chemical monitoring [Review]. In: Brown PR, Grushka E, eds. Advances in chromatography. New York: Marcel Dekker, 1993:1–66.
8. Koutny LB, Schmaizing D, Taylor TA, Fuchs M. Microchip electrophoretic immunoassay for serum cortisol. Anal Chem 1996;68: 18–22.
9. Kricka LJ, Wilding P. Micromachining. A new direction for clinical analyzers. Pure Appl Chem 1996;68:1831–6.
10. Kricka LJ, Faro I, Heyner S, Garside WT, Fitzpatrick G, Wilding P. Micromachined glass-glass microchips for in vitro fertilization. Clin Chem 1995;41:1358–9.
11. Song MI, Iwata K, Yamada M, Yokoyama K, Takeuchi T, Tamlya E, Karube I. Multisample analysis using an array of microreactors for an alternating-current field-enhanced latex immunoassay. Anal Chem 1994;66:778–81.
12. Wilding P, Shoffner MA, Kricka LJ. PCR in a silicon microstructure. Clin Chem 1994;40:1815–8.
13. Northrup MA, Ching MT, White RM, Watson RT. DNA amplification with a microfabricated reaction chamber. In: Digest of technical papers: Transducers 1993 (Proc. 7th int. conf. on solid-state sensors and actuators). New York: Institute of Electrical and Electronic Engineers, 1193:924–6.
14. Jacobson SC, Hergenröder R, Koutny LB, Warmack RJ, Ramsey JM. Effects of injection schemes and column geometry on the performance of microchip electrophoresis devices. Anal Chem 1994;66:1107–13.
15. Jacobson SC, Hergenröder R, Moore AW, Ramsey JM. Precolumn reactions with electrophoretic analysis integrated on a microchip. Anal Chem 1994;66:4127–32.
16. Fluri K, Fitzpatrick G, Chiem N, Harrison DJ. Integrated capillary electrophoresis devices with an efficient postcolumn reactor in planar quartz and glass chips. Anal Chem 1996;68:4285–90.
17. Jacobson SC, Ramsey JM. Integrated microdevice for DNA restriction fragment analysis. Anal Chem 1996;68:720–3.
18. von Heeren F, Verpoorte E, Manz A, Thormann W. Micellar electrokinetic chromatography separations and analyses of biological samples on a cyclic planar microstructure. Anal Chem 1996;68:2044–53.
19. Colyer C, Mangru SD, Harrison DJ. Microchip-based capillary electrophoresis of human serum proteins. J Chromatogr A 1997; 781:271–6.
20. Li PCH, Harrison DJ. Transport, manipulation and reaction of biological cells on-chip using electrokinetic effects. Anal Chem 1997;69:1564–8.
21. Woolley AT, Hadley D, Landre P, deMello AJ, Mathies RA, Northrup MA. Functional integration of PCR amplification and capillary electrophoresis in a microfabricated DNA analysis device. Anal Chem 1996;68:4081–6.
22. Nielsen RG, Rickard EC, Santa PF, Sharknas DA, Sittampalam GS. Separation of antibody-antigen complexes by capillary zone electrophoresis isoelectric focusing and high-performance size-exclusion chromatography. J Chromatogr A 1991;539:177–85.
23. Chen F-TA, Pentoney SL. Characterization of digoxigenin-labeled B-phycoerythrin by capillary electrophoresis with laser-induced fluorescence. Application to homogeneous digoxin immunoassay. J Chromatogr A 1994;680:425–30.
24. Schultz NM, Huang L, Kennedy RT. Capillary electrophoresis-based immunoassay to determine insulin content and insulin secretion from single islets of Langerhans. Anal Chem 1995;67: 924–9.
25. Dirks JL. Diagnostic blood analysis using point-of-care technology [Review]. AACN Clin Issues 1996;7:249–59.
26. Seiler K, Fan ZH, Fluri K, Harrison DJ. Electroosmotic pumping and valveless control of fluid flow within a manifold of capillaries on a glass chip. Anal Chem 1994;66:3485–91.
27. Effenhauser CS, Manz A, Widmer HM. Glass chips for high-speed capillary electrophoresis separations with submicrometer plate heights. Anal Chem 1993;65:2637–42.
28. Branebjerg J, Fabius B, Gravesen P. Application of miniature analyzers: from microfluidic components to μTAS. In: van den Berg A, Bergveld P, eds. Micro total analysis systems. Dordrecht, The Netherlands: Kluwer Academic Publishers, 1995:141–51.
29. Jorgenson JW, Lukacs KD. Zone electrophoresis in open-tubular glass capillaries. Anal Chem 1981;53:1298–1302.
30. Crank J. The mathematics of diffusion, 2nd ed. Oxford: Clarendon Press, 1975:14–6.
31. Sober HA, ed. Handbook of biochemistry. Selected data for molecular biology, 2nd ed. Cleveland, OH: CRC Press, 1970:C-11.
32. Jolley ME, Stroupe SD, Schwenzer KS, Wang CJ, Lu-Steffes M, Hill HD, et al. Fluorescence polarization immunoassay. III. An automated system for therapeutic drug determination. Clin Chem 1981;27:1575–9.
33. Loomis KF, Frye RM. Evaluation of the Abbott TDx™ for the stat measurement of phenobarbital, phenytoin, carbamazepine, and theophylline. Am J Clin Pathol 1983;80:686–91.
34. McCormick RM, Nelson RJ, Alonso-Amigo MG, Benvegnu DJ, Hooper HH. Microchannel electrophoretic separations of DNA in injection-molded plastic substrates. Anal Chem 1997;69:2626–30.
35. Effenhauser CS, Bruin JM, Paulus A, Ehrat M. Integrated capillary electrophoresis on flexible silicone microdevices: analysis of DNA restriction fragments and detection of single DNA molecules on microchips. Anal Chem 1997;69:3451–7.